

Artificial Cells, Nanomedicine, and Biotechnology

An International Journal

ISSN: (Print) (Online) Journal homepage: www.tandfonline.com/journals/ianb20

Human tendon stem/progenitor cell-derived extracellular vesicle production promoted by dynamic culture

Marta Clerici, Maria Camilla Ciardulli, Erwin Pavel Lamparelli, Joseph Lovecchio, Emanuele Giordano, Tina P. Dale, Nicholas R. Forsyth, Nicola Maffulli & Giovanna Della Porta

To cite this article: Marta Clerici, Maria Camilla Ciardulli, Erwin Pavel Lamparelli, Joseph Lovecchio, Emanuele Giordano, Tina P. Dale, Nicholas R. Forsyth, Nicola Maffulli & Giovanna Della Porta (2025) Human tendon stem/progenitor cell-derived extracellular vesicle production promoted by dynamic culture, *Artificial Cells, Nanomedicine, and Biotechnology*, 53:1, 1-16, DOI: [10.1080/21691401.2025.2475099](https://doi.org/10.1080/21691401.2025.2475099)

To link to this article: <https://doi.org/10.1080/21691401.2025.2475099>



© 2025 The Author(s). Published by Informa UK Limited, trading as Taylor & Francis Group



Published online: 10 Mar 2025.



Submit your article to this journal [↗](#)



Article views: 312



View related articles [↗](#)



View Crossmark data [↗](#)

after injury relatively limited [3]. Early and intense inflammatory responses frequently result in the formation of adhesions and scars [4], which, in turn, can compromise tendon strength and increase the risk of re-injury [5]. Therefore, it is crucial to modulate anti-inflammatory strategies and the prevention of scar formation in treating tendon injuries [6].

There has been a recent growing interest in the study of tendon stem cells (TSPCs), a progenitor cell population residing in tendon tissue [7]. TSPCs possess stem cell-like properties, including self-renewal capabilities, multi-differentiation potential, and the ability to form cell colonies [8]. Growing studies have shown their applications in tissue engineering, as *in vitro* models to study tenogenic regenerative events [9–13], in combination with specific growth factors, such as growth differentiation factor-5 (GDF-5), which plays a role in tendon repair and maintenance [14]. GDF-5 induces tenogenic differentiation in different types of stem cells, such as adipose-derived [15,16], umbilical cord-derived [17], and bone marrow-derived mesenchymal stem/stromal cells (MSCs) [18].

Furthermore, the cell's immediate microenvironment, or niche, is crucial to promote adequate function of stem cells. In this respect, Extracellular Vesicles (EVs) have been reported as micro- and nano-scale membrane vesicles actively released by cells, both in healthy states and during pathological conditions [19]. Initially considered cellular debris [20], EVs play a pivotal role as messengers for intercellular communication and are valuable biomarkers for diagnosing and predicting diseases [21] since they can carry genetic information [22–25] and play a crucial role in both inflammation [25–27] and tissue repair. Adopting EVs and/or their constituents, such as proteins and lipids, in new therapeutic formulations to address tendon disorders may offer the advantage of reduced likelihood of immune responses, lower cytotoxicity side effects, and mitigation of post-implantation risk [25,28]. Recent reports have highlighted the potential of EVs derived from different cell types in regenerative medicine for tendinopathy. Bone marrow mesenchymal stem cells (MSCs) have been shown to promote proliferation, migration and fibrotic activity of TSPCs [29,30], as well as promote angiogenesis and inhibit inflammation in damaged tissues [31,32]. Adipose-derived stem cells (ASCs) derived EVs have been reported to attenuate inflammatory response and promote intrinsic healing [16,33,34]. However, the involvement of EVs derived from TSPCs in tendon regenerative processes is an ongoing investigation. Previous studies have isolated and characterised TSPCs-derived EVs from rats [6,8,35], but no reports, to the best of our knowledge, have done it on human TSPCs-derived EVs.

Moreover, previous reports have shown that the dynamic culture, through bioreactor systems, offers superior conditions for the production of extracellular vesicles (EVs) [36–41]. Data indicated that dynamic environments, characterised by continuous agitation or perfusion, result in higher EV yields compared to static cultures. The dynamic conditions facilitate more efficient distribution of nutrients and oxygen throughout the culture, leading to improved cell viability and productivity [42]. Furthermore, dynamic culture systems help alleviate challenges such as sedimentation and cell clumping, which

can hinder EV production in static cultures. Overall, these findings emphasise the importance of dynamic culture techniques in optimising the efficiency and scalability of EV bioprocessing within bioreactor settings [38].

In the present study, we have successfully extracted and characterised human TSPCs and demonstrated the efficiency of GDF-5-supplemented media in promoting a tenogenic activity in TSPCs. Moreover, we investigated the isolation and characterisation of their EVs in two different culture conditions, which, to the best of our knowledge, has not been done before. For EV isolation, we selected ultracentrifugation due to its ability to provide a balance between yield and purity, which is essential for reliable EV analysis. Compared to alternative methods like size-exclusion chromatography (SEC) and precipitation, ultracentrifugation is particularly effective for processing larger volumes of conditioned media, as required in dynamic culture systems. While SEC can yield highly pure EV fractions, it may offer a lower yield, and precipitation methods, though efficient and user-friendly, often result in the co-isolation of non-vesicular proteins, potentially affecting EV purity. Thus, ultracentrifugation was chosen as a practical method for achieving consistent and high-purity EV preparations suitable for downstream analyses [43]. Additionally, we showed that dynamic culture in perfusion appeared to be more effective for EV production and collection. The presence of EVs was confirmed through morphological analysis (SEM, TEM and Nanosight), as well as related protein content assays. A more comprehensive understanding of the mechanisms by which EVs promote tendon repair is crucial for advancing EVs as a novel therapeutic approach for addressing new drug delivery formulation for tendon disorders.

Materials and methods

Isolation and culture of human TSPCs

TSPCs were isolated from biopsies of healthy human semitendinosus tendons following an already published protocol under previously granted Ethical Approval [9]. A total of three healthy semitendinosus samples were acquired from male donors aged 25, 51, and 70, following informed consent. In detail, samples of tendons were obtained from non-suitable tissue sections typically discarded during the procurement of semitendinosus autologous transplants for anterior cruciate ligament reconstruction. The presence of comorbidities or any previous or concurrent anterior cruciate ligament disease were considered exclusion criteria. The isolation of TSPCs was performed as follows: the tendon samples were initially rinsed thrice with sterile phosphate-buffered saline (PBS) (LONZA®, BE17-516F) containing 1% Penicillin-Streptomycin (P-S) (Corning) and 1% Amphotericin B (Ampho B) (Corning). Following the washing process, the tissue was sectioned into small fragments, ensuring the removal of any visible muscle or fat, and placed into pre-scratched Petri dishes. 3ml of 0.25% trypsin–2.21 mM EDTA in 1X solution (Corning, 25051) was added to each dish and then incubated at 37°C for 30 min. Subsequently, the enzymatic action was neutralised using 12 ml of α -MEM (Corning, 15012CV) supplemented with

1% Glutagro™, 1% P-S, 1% Ampho B, and 10% Foetal Bovine Serum (FBS). Culture media was changed weekly until the migration of TSPCs from the tendon pieces to the culture plate happened. When TSPCs reached 50% confluence the tissue pieces were discarded, and fresh media was added. When TSPCs reached 80% confluence, they were detached using trypsin-EDTA and centrifuged at 1400rpm for 10min. TSPCs were cultured for 120days, and at different passages (P3 and P16), cells were collected for qRT-PCR and flow cytometric analysis.

Multipotent differentiation

Multipotent differentiation (adipogenic, chondrogenic and osteogenic) was performed as previously reported [44]. The experiment was performed on early passage (P3) and late passage (P16) TSPCs; cells were seeded at 5000 cells/cm² and cultured for 28days in differentiation induction medium. The adipogenic medium comprised high glucose DMEM (Corning) supplemented with L-glutamine and enriched with 0.1µM dexamethasone (Sigma Aldrich, D2915), 0.5mM 3-Isobutyl-1-methylxanthine (Sigma Aldrich, I5879), 10mg/ml human insulin solution (Sigma Aldrich, I9278), 100µM indomethacin (Sigma Aldrich, I7378), 10% FBS, 1% non-essential amino acids (NEAA), 1% Penicillin-Streptomycin (P-S), and 1% Amphotericin B (Ampho B). The chondrogenic media consisted of high glucose DMEM with L-glutamine supplemented with 1% v/v Insulin-Transferrin-Selenium (Gibco™, 41400045), 0.1µM dexamethasone, 50µM ascorbic acid, 40µg/ml L-proline, 1% sodium pyruvate (Gibco™, 11360070), 10ng/ml Recombinant human TGF-β3 (Peprotech, 100-36E), 1% v/v FBS, 1% NEAA, 1% P-S, and 1% Ampho B. The osteogenic medium comprised high glucose DMEM with L-glutamine supplemented with 50µM ascorbic acid (Sigma Aldrich, A4544), 10µM β-glycerophosphate (Sigma Aldrich, G9422), 0.1µM dexamethasone, 10% FBS, 1% NEAA, 1% P-S, and 1% Ampho B. The control medium consisted of high glucose DMEM with L-glutamine supplemented with 10% FBS, 1% NEAA, 1% P-S, and 1% Ampho B.

Cells were seeded on day -1 in the control culture medium to allow cells to adhere and have the same starting point for all the conditions. After 24h, at day 0, the control medium was replaced with differentiation media. Media changes occurred twice a week, and at each time point (day 0, 7, 14, 21 and 28), some cells were fixed with 4% paraformaldehyde and stored at 4°C with PBS. Histological staining procedures involved using 3mg/ml Oil Red O (Sigma Aldrich, O0625-100G) in 99% isopropanol for adipogenesis, 1% Alcian blue 8GX (Sigma Aldrich, A3157-10G) in 0.1M aqueous HCl for chondrogenesis, and 2% alizarin red S sodium salt (Alfa Aesar, 42040) in distilled water (dH2O) for osteogenesis. Images were captured using a Leica DMIL LED microscope and acquired with a Leica DFC425 C Camera.

Flow cytometry analysis

TSPCs, both early (P3) and late passage (P16), were detached and 50,000 cells were taken for staining performed as

follows. After successive washes in 1x PBS, cells were briefly incubated at room temperature (RT) for 20min with the following directly conjugated mouse-anti-human antibodies: CD34-PE (A07776), CD90-FITC (IM1839U), CD105-PE (A07414), CD45-PC7 (IM3548), Anti-HLA-DR-FITC (IM0463U), and CD14-PC7 (A22331) (all from Beckman Coulter), along with CD73-APC (Miltenyi Biotech, 130-095-183). Following the antibody incubation, samples underwent two washes with 1x PBS and were then resuspended in the same buffer for acquisition. The acquisition was performed using a BD FACSVerse™ flow cytometer (Becton Dickinson) equipped with two lasers (blue: 488nm and red: 628nm). A minimum of 30,000 events were recorded. Post-acquisition compensation and analysis were conducted using Kaluza software (v.2.1, Beckman Coulter). Flow cytometry events were initially gated by plotting forward scatter (FSC) versus side scatter (SSC), followed by the exclusion of double cells (FSC-A vs. FSC-H), before determining CD surface marker expression.

Growth rate analysis

To determine if the growth rate was affected by the ageing process, cells underwent a 120-day culture period. Population doublings (PDs) were computed utilising the formula $PD = \log_{10}(N/N_0)/\log_{10}(2)$, where 'N' represented the count of harvested cells at the passage, and 'N₀' denoted the initial cell count. These values were then utilised to derive the cumulative population doublings (CPDs) over time using the formula $CPD_n = PD_0 + PD_n + PD_{n-2}$ (where 'n' corresponds to the time point, equivalent to the days in culture). Subsequently, these CPD values were employed to construct a growth curve, with the X-axis representing the time points and the Y-axis depicting CPD values. The same type of analysis has been previously reported [44].

Morphological analysis

Images of TSPCs were captured at different passages (P3 and P16) with a Leica DMIL LED microscope (Leica DFC425 C Camera) and were subjected to analysis for aspect ratio. The analysis was performed to show possible changes in human TSPC phenotype over time, and this approach has already been validated in previous studies [17,44]. The ImageJ analysis software [45] was utilised, employing its manual tool to delineate the perimeter of cells. Subsequently, the aspect ratio was computed by dividing the major axis length (length) of the cell area by the minor axis length (width). Thirty individual cells were randomly chosen across three image fields for analysis.

RNA extraction and gene expression by RT-qPCR

RNA extraction was performed with the RNeasy Micro kit (Qiagen, 74004) according to the manufacturer's instructions. The concentration of the extracted RNA was quantified using a Nanophotometer NP80 (Implen™). Then, the iScript™ cDNA synthesis kit (Bio-Rad, 1708891) was used to reverse-transcribe

1 µg of total RNA for each sample through a Thermal Cycler 2720 instrument (Applied Biosystems). RT-qPCR was undertaken using the SsoAdvanced™ Universal SYBR® Green Supermix (Bio-Rad, 1725271) and the validated primers for SCX-A, DCN, TNC, COL1A1, COL3A1 (Bio-Rad), and TNMD (Sigma), according to MIQE guidelines [46]. It was performed on a LightCycler® 480 Instrument (Roche). Triplicate experiments were performed for each condition studied, and data were normalised to GAPDH expression (Bio-Rad). Fold changes were determined using the $2^{-\Delta\Delta Ct}$ method and presented as relative levels over Early passage = 1 and T0=1.

Immunofluorescence assay

Cells underwent fixation with 4% paraformaldehyde for 30 min at room temperature (RT), followed by permeabilisation using 0.1% Triton X-100 for 10 min. Subsequently, cells were treated with a blocking buffer consisting of 1% bovine serum albumin (BSA) and 0.1% Tween 20 for 1 h. For staining of type I collagen and TNMD, cells were incubated overnight at 4°C with mouse monoclonal anti-type I primary antibody (1:100; Sigma Aldrich, MAB3391) and rabbit polyclonal anti-TNMD primary antibody (1:100; Abcam, ab203676), respectively. After primary antibody incubation, cells were treated for 1 h at RT with Alexa Fluor™ 594 goat-anti-mouse IgG (1:500; Thermo Fisher Scientific, A-11005) and Alexa Fluor™ 488 goat-anti-rabbit IgG (1:500; Thermo Fisher Scientific, A-11008) antibodies. Cell nuclei were stained with 4',6-diamidino-2-phenylindole (DAPI) solution (1:1000; Sigma Aldrich, D9542) for 5 min at RT. Imaging was conducted at 20× magnification with consistent settings for light, exposure time, and gain using a fluorescence microscope (Eclipse Ti Nikon Corporation).

GDF-5 treatment

To evaluate the effect of GDF-5 supplemented media on TSPCs, P3 cells were seeded at 5000 cells/cm² and cultured for 28 days in the tenogenic medium. The medium consisted of high glucose DMEM with L-glutamine supplemented with 50 µM ascorbic acid (Sigma Aldrich, A4544), 100 ng/ml recombinant human GDF-5 (Peprotech, 120-01), 10% FBS, 1% NEAA, 1% P-S and 1% Ampho B. Control media was previously described for multipotent differentiation. Cells were seeded on day -1 in the control culture medium. After 24h, at day 0, control media were replaced with differentiation media, where appropriate, for day 7, 14, 21 and 28-time points. Media were changed twice a week, and at each time point, cells were fixed with 4% paraformaldehyde and stored at 4°C with PBS. Cells cultured in tenogenic media and their controls were also collected for qRT-PCR and immunofluorescence (IF) assays. After 28 days, 0.1% Sirius red (Sigma-Aldrich, 365548) in picric acid was used for histological staining.

TSPCs static and dynamic culture

For static conditions, TSPCs were seeded into 2T-175 cm² flasks with 30 ml of GDF-5-supplemented media in each. For dynamic stimulation, a customised perfusion device operating

within a standard cell culture incubator was used. The apparatus was composed of 2T-175 cm², each featuring holes allowing the insertion of 2 needles (20G, BD Microlance™, 301300) connected with silicon tubes (Tygon®) providing perfusion *via* peristaltic pumps at a constant flow rate of 1 ml/min (Figure 3a). The dynamic culture conditions had already been optimised in previous studies [42,47,48] to ensure effective metabolite and oxygen transfer without imposing significant shear stress on the cells. This flow rate was selected to maintain high cell viability and stable primary cell culture, as higher flow rates in preliminary trials resulted in cell detachment and apoptosis. In both culture conditions, TSPCs were seeded at a density of 5000 cells/cm² in GDF-5 supplemented media. The medium was continuously recirculated within the flasks under dynamic culture and replaced twice a week. In both culture conditions, culture duration was the same (usually one week), until they reached 80% confluence. Both setups were maintained under identical environmental conditions (e.g. temperature, medium replacement schedule, same culture duration), ensuring a fair comparison between static and dynamic conditions.

Finite element modelling (FEM) analysis

Finite Element Modelling (FEM) was implemented using COMSOL Multiphysics Software to assess medium velocity distribution within the culture plate. Laminar flow was modelled for dynamic conditions, where the plate was obtained using a rectangular geometry (length = 137 mm, width = 116 mm, and height = 11 mm) and inlet/outlet using a cylindrical geometry (diameter = 0.6 mm and height = 40 mm). At steady-state conditions, the medium velocity distribution was simulated considering a flow rate of 1 ml/min (i.e. an inner velocity of 0.06 m/s). A sensitivity study of the mesh addressed the most computationally efficient solution.

TSPCs starvation and conditioned media collection

When TSPCs reached 80% confluence, they were washed for two minutes in PBS and then switched to a serum-free standard basal culture media for 24 h to facilitate the collection of EVs. After 24h, 30 ml of conditioned media were collected from each T-175 flask, filtered using 0.22 µm syringe filters, and then frozen at -20°C. After collecting the media, cells were washed with PBS, enzymatically detached using trypsin-EDTA and frozen at -80°C. Some samples were used for Western blot analysis.

EVs isolation

EV isolation was performed using the ultracentrifugation method, following a protocol reported elsewhere [49,50]. Conditioned media was thawed and transferred to centrifuge tubes (Beckman Coulter, Open-Top Thick wall ultra-Clear Tube, 355631), then spun down using a swinging bucket rotor SW31.1 Ti (Beckman Coulter, 369651). Centrifugation conditions were set as 100000G for 90 min, using the Optima™ XE-100 ultracentrifuge (Beckman Coulter, A94516). The

resulting supernatant was discarded and, the EV pellets from static and dynamic cultures were resuspended in 1 ml of distilled water (dH₂O) to perform further analysis.

Protein concentration

The total protein concentration of the EV pellets was analysed using Pierce™ Bradford Plus Protein Assay Reagent (Thermo Scientific™, 23238) according to the manufacturer's instructions.

Nanoparticle tracking analysis (NTA)

The size and concentration of nanoparticles in the EV pellets were assessed using the Nanosight NS300 nanoparticle characterisation system (Nanosight Ltd), equipped with fast video capture and particle-tracking software. Samples were not diluted and were injected into the laser chamber at a constant rate, controlled by a syringe pump. Three recordings were performed for each sample. Nanoparticle Tracking Analyse (NTA) software was used to measure the size, expressed as mean ± SD size distribution, and the concentration of nanoparticles. The batch process included in the software was used to integrate the three technical measurements of each sample.

EV morphology

The morphology of EVs was investigated using a Field Emission-Scanning Electron Microscope (FE-SEM model LEO 1525, Carl Zeiss SMT AG, Oberkochen, Germany). To prepare the samples, several droplets were placed onto an aluminium stub using double-sided adhesive carbon tape and subsequently dried using a critical point drier (model K850, Quorum Technologies Ltd, East Sussex, United Kingdom). A thin layer of gold film (with a thickness of 250 angstroms) was then applied to the samples using a sputter coater (model 108A; Agar Scientific, Stansted, UK). To capture TEM micrographs, 10 µl of each vesicle suspension was applied onto a formvar/carbon 200 mesh copper grid (Ted Pella, USA Cat. No. 01800-F) and allowed to air dry for several hours. The resulting images were acquired using a transmission electron microscope (TEM) in bright-field mode, specifically the FEI TECNAI G2 200kV S-TWIN microscope equipped with a 4K camera (electron source with LaB₆ emitter; FEI Company, Dawson Creek Drive, Hillsboro, OR, USA). Bright-field (BF) TEM images were captured at 120kV using a spot size of 3 and an integration time of 1 s.

Western blot

Starved TSPCs, cultured in both static and dynamic conditions, were thawed in fresh media, spun down for 15 min at 1400 rpm, resuspended in 1 ml PBS and then lysed in RIPA buffer ((1:4) (NaCl 150 mM, 1% Triton X-100 pH 8.0, 0.5% sodium deoxycholate, 0.1% SDS, 50 mM Tris, pH 8.0), supplemented with protease inhibitors cocktail and phosphatase

inhibitors (Merck)) for 45 min on ice, shaking the samples every 10 min. Cell lysates were then centrifuged for 20 min at 15,000× *g*, and the supernatants were transferred to a new 1.5 ml tube. Protein content was determined by BCA assay (Thermo Scientific™, 23225), and 25 µg of total protein was loaded per lane. EV pellet proteins were determined by Bradford assay, and the total amount was resuspended in 100 µl of distilled water and then equally split between all the lanes. Then, protein extracts were separated by SDS-PAGE gels and transferred onto nitrocellulose membranes. Nitrocellulose blots were blocked with 10% non-fat dry milk in TBS-T buffer (20 mM Tris-HCl, pH 7.4, 500 mM NaCl and 0.1% Tween-20) and incubated in TBS-T buffer containing 5% BSA overnight at 4 °C with the following primary antibodies (all diluted 1:1000): anti-Calnexin (ab133615), anti-CD9 (ab263019), anti-CD63 (ab134045), anti-CD81 (ab109201), anti-Hsp70 (ab181606), anti-TSG101 (ab125011), provided from Abcam and anti-α-tubulin (T5168) supplied by Sigma Aldrich. Immunoreactivity was detected by sequential incubation with appropriate HRP-conjugated secondary antibodies (Biorad, 1706515) for 1 h at RT and Pierce™ ECL Western blotting substrate (Thermo Scientific, 32106) on a radiography film. Densitometry of bands was performed with ImageJ software (version 1.53c). The area under the curves, each relative to a band, was determined, and the local background was subtracted from the calculated values.

Multiplex surface marker analysis

The flow cytometric analysis involved the use of the MACSplex Exosome Kit designed for human samples (Miltenyi Biotec, 130-122-209), which detects 37 exosomal surface epitopes, along with two isotype controls. The analysis was performed following the manufacturer's instructions. Briefly, EV-containing samples were mixed with MACSplex buffer (MPB) to reach a final volume of 120 µL. These mixtures were loaded into 1.5 ml tubes, along with 15 µL of MACSplex Exosome Capture Beads. The tubes were incubated overnight at RT on an orbital shaker (450 rpm), protected from light. After the incubation, 500 µL of MPB was added to each tube, followed by centrifugation at RT at 3000× *g* for 5 min. The supernatant was carefully removed, and 5 µL of MACSplex Exosome Detection Reagent CD9, CD63, and CD81 were added to each tube. Samples were incubated for 1 h at RT in an orbital shaker (450 rpm). After the incubation, the tubes underwent another washing step, involving the addition of 500 µL of MPB to each tube, followed by a 15-minute incubation at RT in an orbital shaker (450 rpm). The EV-containing samples were centrifuged again, and the supernatant was discarded, leaving about 200 µL in each tube. Flow cytometric analysis was carried out using a BD FACSVerser™ flow cytometer (Becton Dickinson) by acquiring 5,000 events, followed by data analysis with Kaluza software (v.2.1, Beckman Coulter).

Statistical analysis

Statistical analysis was carried out with GraphPad Prism software (version 9.4.1). The data, which was collected from multiple experiments (*n*=3), is presented as the mean ± SD. To

assess statistical significance among independent groups, the Mann-Whitney test and t-test have been applied. Flow cytometry data were reported as the percentage of positive cells for TSPCs characterisation (Figure 1a) or as the median fluorescence intensity (MFI) of each EV marker for MACS Plex data analysis (Figure 5c). For the latter, the background was subtracted from samples using the median MFI values of each marker obtained from three different controls: PBS alone, MACS Plex buffer alone, and PBS+MACS Plex buffer. Next, a single median MFI value from CD9, CD63, and CD81 was calculated for each sample, and

a median value for dynamic and static condition samples was calculated. These values were used for data normalisation, as the MFI value of each marker was divided by the normaliser for dynamic or static conditions. Surface marker concentrations below the corresponding control antibody included in the kit, which serves as a measurement threshold, were considered negative results. MACS Plex results were also visualised by heatmap with dendrograms using RStudio software (v.2022.07.1; RStudio, Boston, MA, USA). Differences were regarded as statistically significant when the p-value was less than 0.05.

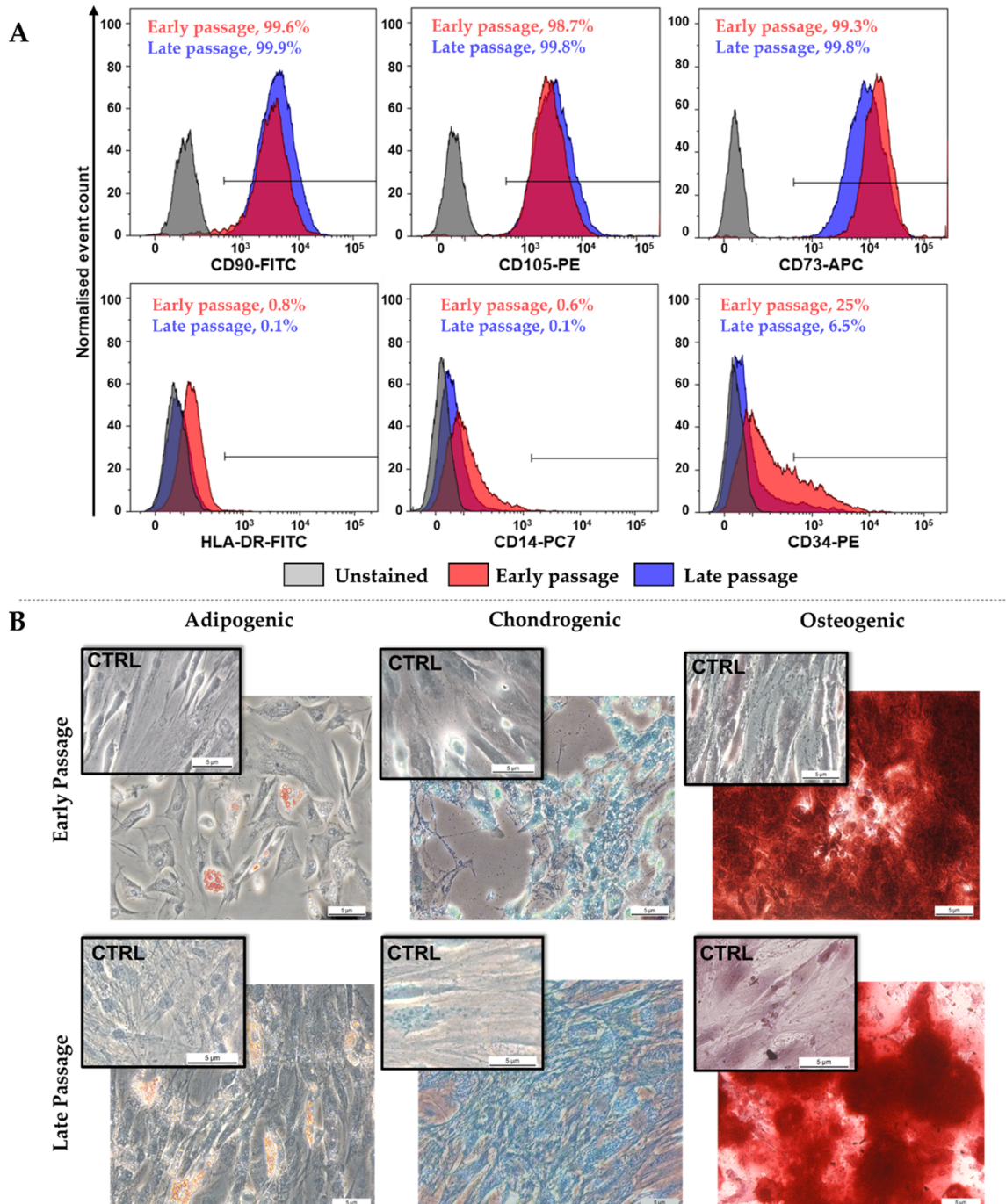


Figure 1. Testing of stemness properties of TSPCs at an early (P3) and late passage (p16). (A) flow cytometry analysis of the CD90, CD105, CD73, HLA-DR, CD105, and CD34 surface marker expression of TSPCs. Normalised cell count histograms display marker expression on single cells. (B) The multipotency of TSPCs has been proved through histological assays by adipogenic, chondrogenic, and osteogenic differentiation. Scale bar = 5 μm.

Results

TSPCs isolation and characterisation

Human TSPCs were extracted from healthy semitendinosus tendon tissue samples using an explant method [9], harvested and characterised by flow cytometry, and their multipotency potential was tested at an early (P3) and late passage (P16).

Flow cytometry analysis

TSPCs were positive for the typical MSC surface markers CD90, CD73 and CD105 and negative for HLA-DR, CD14, and CD34 by flow cytometry. This immunophenotype profile was largely retained across different passages (from P3 to P16), as no significant variations were described, except for a decrease in CD34 from 25% positive cells at early passage to 6.5% at P16 (Figure 1a).

Multipotent differentiation

TSPCs displayed multipotency potential in early and late passage cells, staining positively for histological stains: Oil red O for adipogenesis, Alcian blue for chondrogenesis and Alizarin red for osteogenesis, following 28 days of exposure to differentiation media (Figure 1b). Visual inspection suggested that low efficiency of differentiation into adipocytes and osteocytes was obtained in later passage cells compared to earlier passage.

Morphological and growth rate analysis

TSPCs morphological investigation indicated a 1.1-fold decrease ($p < 0.0001$) in the aspect ratio measurement, showing that cells were becoming larger and flatter, as can be observed from visual inspection in bright-field images (Figure 2a). The cell growth rate was measured for TSPCs cultured for 120 days and it was shown that that cells displayed continuous proliferation over the whole culture time, achieving 29.6 CPD without entering the growth plateau stage (Figure 2b).

Gene expression

TSPCs gene expression profile was measured across different passages, and the results showed that all tested tenogenic genes (SCX-A, DCN, TNC, TNMD and COL3A1) were down-regulated in late passage compared to the early passage cells, in most cases also significantly, such as SCX-A (20-fold decrease, $p < 0.05$), DCN (2-fold decrease, $p < 0.05$), TNC (3.4-fold decrease, $p < 0.05$) and COL3A1 (1.5-fold decrease, $p < 0.05$) (Figure 2c). The data suggests that the ageing process affected TSPCs tenogenic phenotype.

Evaluation of GDF-5 effect on TSPCs

TSPCs were cultured in GDF-5 supplemented media (100 ng/ml) to evaluate the tenogenic potential of this treatment on TSPCs. After 14 days of culture, TSPCs gained a more elongated

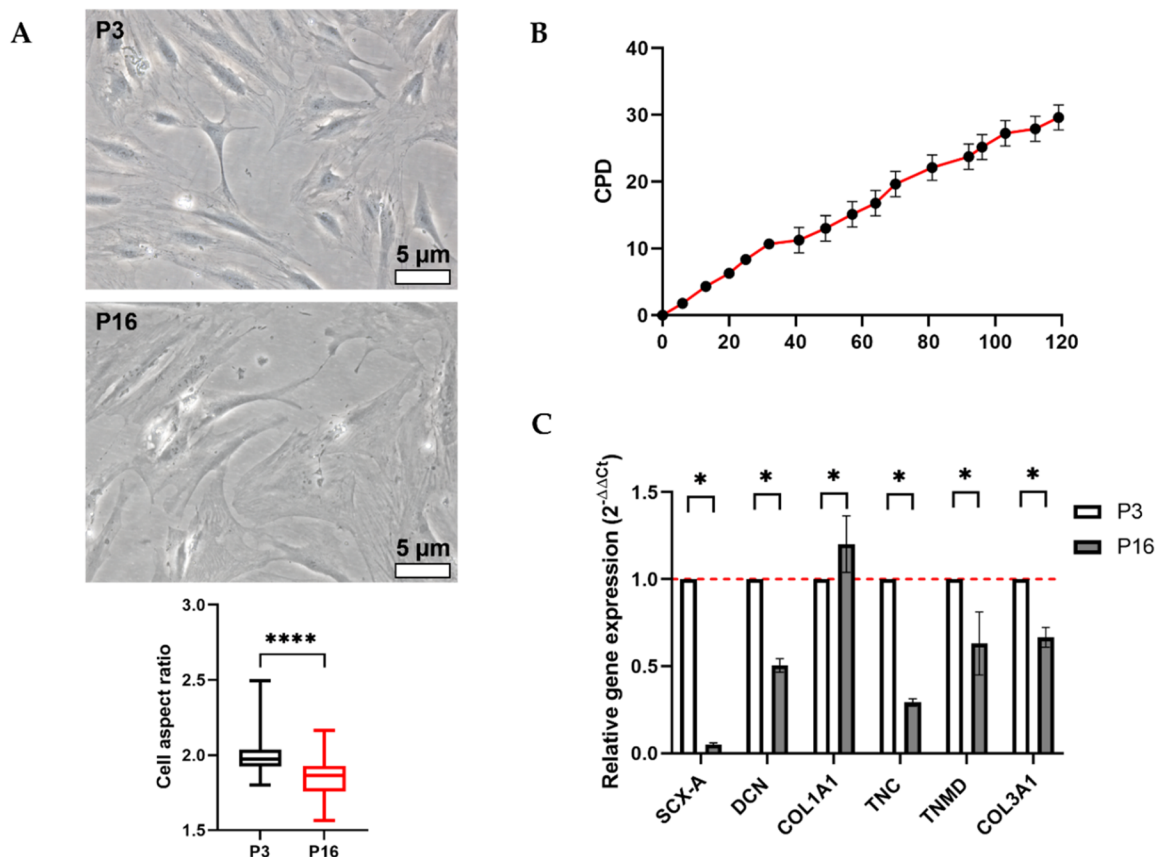


Figure 2. TSPCs morphological, growth and transcriptional characterisation at an early (P3) and late (P16) passage. **(A)** Morphological analysis by bright field microscope and cell aspect ratio measurement. Scale bar = 5 μ m. **(B)** Growth kinetics of TSPCs across 120 days of culture. **(C)** The gene expression profile for tenogenic markers (SCX-A, DCN, COL1A1, TNMD and COL3A1) presented as relative levels over early passage = 1. Data are shown as mean \pm SD. * for $p < 0.05$ ($N=3$).

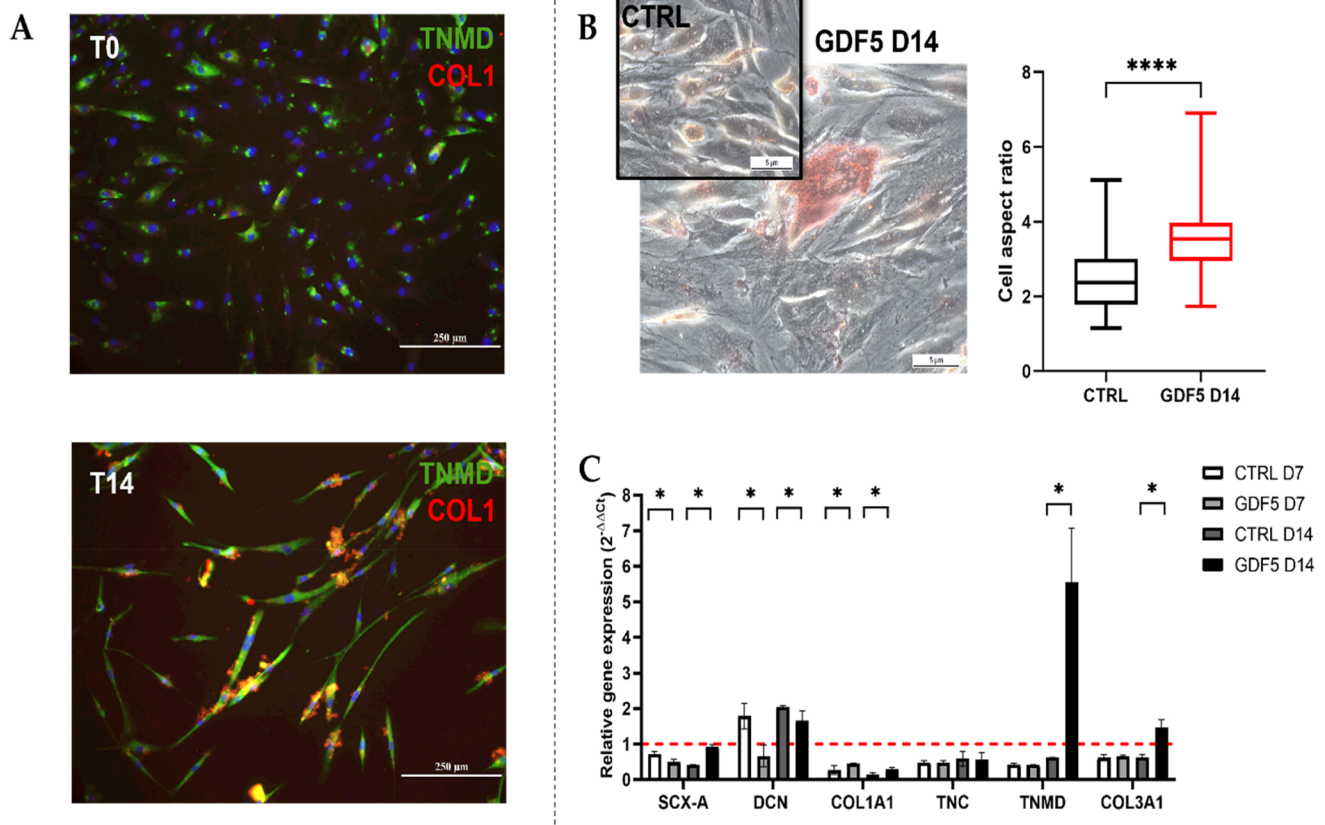


Figure 3. TSPCs were cultured for 14 days in GDF5-supplemented media. **(A)** Immunofluorescence images of TNMD (green) and COL1 (red) at day 0 (D0) and after 14 days of GDF5 treatment (D14). Scale bar = 250 μm . **(B)** Brightfield images of Sirius red staining and morphological analysis performed through cell aspect ratio measurement between CTRL and GDF5 D14 samples. **(C)** Gene expression profile for tenogenic markers (SCX-A, DCN, COL1A1, TNC, TNMD, COL3A1) presented as relative levels over T0=1. Data are shown as mean \pm SD. * $p < 0.05$, **** $p < 0.0001$ ($N=3$).

morphology (tenocyte-like), which was confirmed both from IF pictures (Figure 3a) and cell aspect ratio measurement (Figure 3b), which showed a significant increase (1.5-fold increase, $p < 0.0001$). Visual inspection of IF pictures also showed the increased expression of TNMD (green) and COL1 (red). Moreover, the transcriptional analysis showed that after 7 days of GDF-5 treatment, TSPCs showed a 1.75-fold decrease in SCX-A ($p < 0.05$), a 1.2-fold decrease in DCN ($p < 0.05$) and a 1.7-fold increase in COL1A1 ($p < 0.05$). Conversely, after 14 days of GDF-5 treatment, TSPCs showed a significant upregulation in SCX-A (2.3-fold, $p < 0.05$), COL1A1 (2-fold, $p < 0.05$), TNMD (9-fold, $p < 0.05$) and COL3A1 (2.3-fold, $p < 0.05$) compared to the CTRL (Figure 3c).

TSPCs static and dynamic culture

TSPCs were cultured in GDF-5 supplemented media until they reached 80% confluence, both in static and dynamic conditions, to allow for comparative analysis. In dynamic conditions, a continuous flow rate of 1 ml/min was applied, which provided a uniform medium velocity distribution (horizontal cross-section) with an average value of 8.28×10^{-6} m/s, as determined through finite element method (FEM) analysis (Figure 4b). After 24 h of starvation, cells were detached from both static and dynamic cultures, and cell counting was performed. Results showed that the number of cells from the dynamic culture was consistently higher

than that in the static culture, despite both conditions starting with the same seeding density. Protein expression analysis was conducted on starved cells from both conditions to evaluate EV markers. Western blotting was used to determine protein levels of tetraspanins (CD9, CD63, CD81), along with Calnexin, TSG-101, and HSP-70. Results indicated that TSPCs cultured in static conditions expressed significantly higher CD9 (2.6-fold, $p < 0.0001$), CD63 (1.5-fold, $p < 0.0001$), Calnexin (1.5-fold, $p < 0.001$) and TSG-101 (1.02-fold, $p < 0.05$), while CD81, TSG-101 and HSP-70 protein levels did not show significant differences between the two conditions (Figure 4c).

EVs isolation and characterisation

Morphological and size analysis

SEM of collected EVs showed that the population was polydisperse and included a proportion of sub-200 nm vesicles (Figure 5a). Better visualisation of particles was possible through TEM, which confirmed the presence of particles whose diameter was in the same range and with a round shape (Figure 5b). Particle size and concentration were quantified by NTA, resulting in a particle concentration of 10^6 particles/ml, corresponding to an average size of 128.1 ± 16 nm in static conditions and 139.1 ± 12 nm in dynamic conditions (Figure 5c).

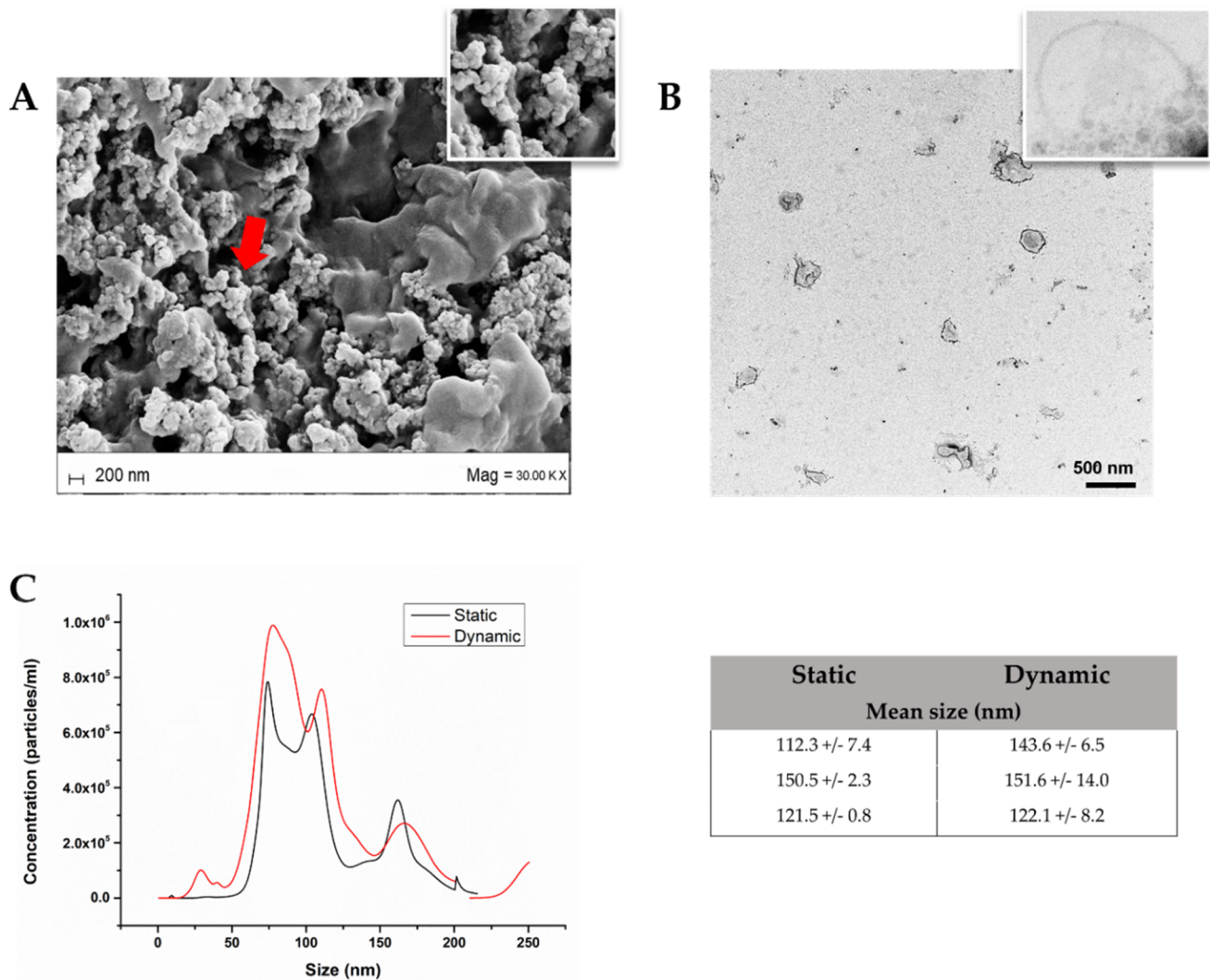


Figure 5. Morphology characterisation of the different extracellular vesicle populations by **(A)** Scanning Electron microscope (SEM), scale bar = 200 nm (zoomed area: 4x magnification); **(B)** Transmission Electron microscope (TEM), scale bar = 500 nm; **(C)** Examples of particle size distribution and concentration observed by NTA ($N=3$).

need to find a consistent source with a stable phenotype, chromosomal abnormalities and genetic instability, host rejection, ectopic tissue development, and tumorigenicity [55]. To overcome these problems, more recently, researchers have investigated the potential of EVs to communicate critical biological information among cells, aiming to transmit the right signals to aid in effective tendon repair [25].

In this study, we have successfully isolated TSPCs from human healthy tendon biopsies using an explant method, following an optimised protocol [9]. We then demonstrated the efficiency of GDF-5 treatment in promoting the maintenance of TSPCs tenogenic profile, which, as we showed, is affected by the cell ageing process. Lastly, we isolated and characterised human TSPCs-derived EVs cultured in two different culture conditions (static and dynamic), which, to the best of our knowledge, had not been performed before.

Consistent with previous reports in human tendon tissues [7,27,56,57], we tested TSPCs stemness properties by showing their multipotent ability to differentiate in other cell types (Figure 1a) and by determining their immunophenotype with positivity for MSC markers (CD73, CD90, and CD105) and

negativity for haematopoietic markers (CD14, CD19, CD34, CD45 and HLA-DR) (Figure 1b), consistent with ISCT guidelines [58]. These properties were retained across different passages, even though, from visual inspection, we could observe a lower efficiency of adipogenic and osteogenic differentiation, as previously reported in other species [44,56,59].

Regarding TSPCs morphology, there is currently a lack of uniformity in their appearance, and their shape changes according to the species [60]. TSPCs exhibit cobblestone-like morphology in rabbits [61] and rats [59], stellate morphology in rats [62], and fibroblast-like morphology in rats and humans [7,63]. Indeed, we report a spindle-shaped morphology, which became flatter and more rounded with proliferative age, with a significant decrease in the aspect ratio measurement (Figure 2a), in agreement with previous reports [61,64,65]. As previously reported [44,59], the proliferative potential of TSPCs was relatively consistent across all passages, and the CPD kept increasing without plateauing during the culture period (Figure 2b). Transcriptional analysis showed downregulation of almost all the tenogenic genes, a probable consequence of the ageing process (Figure 2c), in agreement with

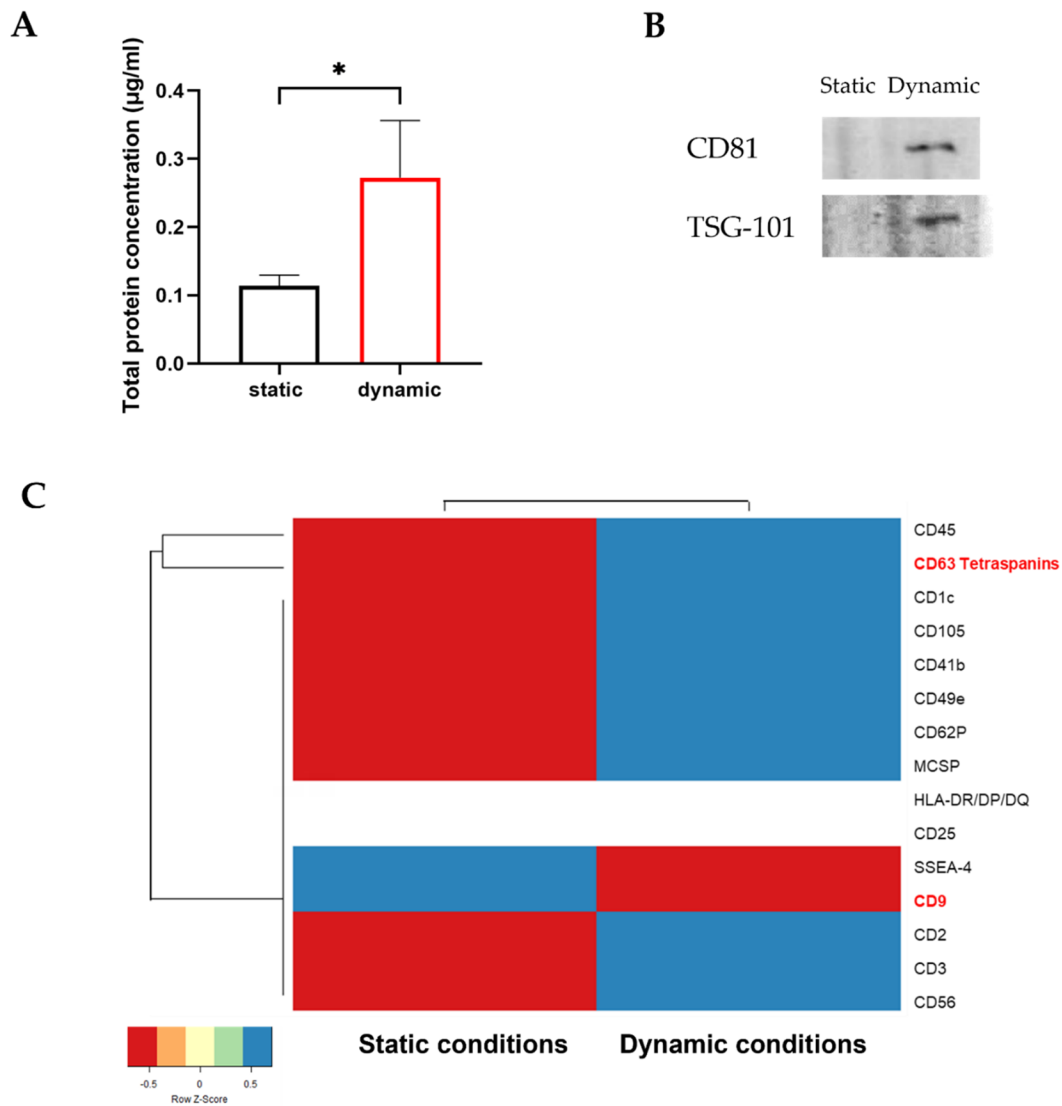


Figure 6. Comparison of EV protein characterisation collected from static and dynamic culture. Total protein concentration was measured by (A) Bradford assay; (B) Western blot analysis of EVs specific markers (CD81, TSG-101); (C) Flow cytometric analysis of exosome surface protein markers. The median APC signal intensity of each specific population of single beads was normalised to the average of the anti-CD9, anti-CD63 and anti-CD81 beads ($N=3$).

Table 1. Flow cytometric analysis of exosome surface protein markers on TSPCs-derived EVs obtained both from static and dynamic culture conditions. Results show that 15 surface markers have been detected: CD45, CD63, CD1c, CD105, CD41b, CD49e, CD62P, MCSP, HLA-DR/DP/DQ, CD25, SSEA-4, CD9, CD2, CD3 and CD56, ($N=3$).

Surface Markers	EVs surface markers expression	
	MFI Values	
	Dynamic	Static
CD63	940	461
CD2	3	0
CD56	4	0
CD3	2	0
CD62P	1	0
CD45	1617	0
CD49e	1	0
CD9	0	1
HLA-DR/DP/DQ	1	1
CD105	1	0
CD1c	1	0
CD25	1	1
SSEA-4	0	1
MCSP	1	0
CD41b	1	0

a previous study which reported the downregulation of SCX-A and TNMD [59].

Given the limited understanding of specific tendon makers and molecular interactions between transcription factors and signalling pathways, there is still a lack of a specific method to efficiently induce tenogenic differentiation of stem cells [66]. To promote a tenogenic commitment of TSPCs and retain their tendon cell phenotype over time, especially as it is affected by the ageing process, as previously demonstrated, we investigated the effect of GDF-5 supplementation. In agreement with previous reports with other stem cell types [15–18], we demonstrated the ability of GDF-5 to promote an enhanced tenogenic profile in human TSPCs, marking, to the best of our knowledge, the first time this has been reported for this specific cell type. The GDF-5 concentration of 100 ng/ml was chosen based on previous optimisations in studies with MSCs from various origins [17]. After 14 days of GDF-5 treatment, TSPCs gained a tenocyte-like shape (Figure 3a and b), maintaining a tendon cell phenotype, as previously

described for murine tendon cells [67], human BM-MSCs [17,68] and WJ-MSCs [17]. Transcriptional analysis showed an increase in key tenogenic markers, including SCX-A, TNMD, and COL3A1 (Figure 3c), supporting a tendon-specific differentiation response. SCX-A increased expression has already been shown in rat tendon stem cells after 14 days of 100 ng/ml GDF-5 supplementation [69]. The same study, as mentioned, focused on the short-term effects of GDF-5 and observed a decrease in TNC and COL1A1 in line with our results. However, some reports have noted peak TNMD and COL3A1 expression at earlier time points, such as 8 days for hBM-MSCs [17] and 6 days for adipose-derived MSCs [70], in contrast with our results, which described 14 days as the most effective time point. This variation highlights cell-type-specific responses to GDF-5 and underscores the need for further research, especially regarding the long-term impact of GDF-5 on TSPC stability, differentiation capacity, and regenerative efficacy. Future studies should examine whether prolonged exposure to GDF-5 can maintain the tenogenic phenotype over extended periods, as this could be crucial for clinical translation.

Together with the biochemical inputs, physical stimuli may be beneficial for tendon development, supporting the mechano-stimulation of cells. In agreement with previous studies, which tested dynamic systems on stem cells, such as bone marrow mesenchymal stem cells [39–42,47,71] and adipose-derived stem cells [72,73], we showed that dynamic conditions could improve current cell culture systems, possibly by better replicating the physiological *in vivo* environment. The present study showed that dynamic conditions, consisting of a custom-made perfusion bioreactor with a continuous flow rate of 1 ml/min, enabling constant nutrient and waste exchange, favoured a more significant protein production of TSPCs-derived EVs. This flow rate was selected to enhance cell viability and EV production while minimising shear stress, as demonstrated in previous optimisation studies. Higher flow rates were tested but led to cell detachment and apoptosis, underscoring the importance of fine-tuning bioreactor parameters for primary cell cultures. To the best of our knowledge, only a few previous studies reported the isolation and characterisation of rat TSPCs-derived EVs [6,8,35], but none of the human TSPCs-derived EVs.

The morphological analysis of human TSPCs-derived EVs, in agreement with previous studies [6,8,35], described sub-200 nm diameter vesicles with a rounded shape, as shown both from SEM and TEM pictures (Figure 5a and b). However, regarding the size distribution, whilst we reported a high concentration of EVs (10^6 particles/ml) approximately at 130–140 nm (Figure 5c), rat TSPCs-derived EVs showed a smaller average vesicle size, below 100 nm [8,35]. Consistent with other studies on other cell types, such as bone marrow MSCs [36] and tumour cell lines [37], in our study, we showed the advantages of using a dynamic culture compared to a static one to allow a larger production of EV protein [74]. Dynamic culture, indeed, provides a consistent flow of nutrients and waste removal, creating a more stable environment that supports cell viability and metabolic activity. This contrasts with static culture, where nutrient and waste gradients can contribute to cellular stress and reduced functionality. Additionally, although the flow rate in our setup was

optimised to minimise shear stress, even low-level mechanical signals from continuous perfusion could subtly influence cellular pathways associated with EV biogenesis. Together, these factors likely create a more favourable environment for EV production. Kang et al. [36], culturing hBM-MSCs in a perfusion bioreactor both with 0.1 ml/min and 1 ml/min flow rates, reported a 5.7-fold and a 7-fold increase in EV protein content obtained from dynamic culture compared to static one, measured with Bradford assay, and we reported a 2.6-fold increase in TSPCs-derived EVs isolated from dynamic culture by using the same assay (Figure 6a). Conversely, in contrast with our results, a previous study from Patel et al. [38], which used a perfusion bioreactor with a flow rate of 4 ml/min to culture human dermal microvascular endothelial cells (HDMECs), showed a 15-fold decrease in total EV protein content obtained from dynamic culture. The observed increase in EV production under dynamic culture conditions may stem from multiple factors inherent to perfusion-based systems. Concerning TSPCs-derived EV protein content, we performed both WB and flow cytometry to test a panel of EV-specific markers, such as tetraspanins, which are involved in many cellular processes, such as cell adhesion, migration and signalling [75]. In agreement with the MISEV 2023 guidelines [76] to define extracellular vesicles, our WB results (Figure 6b) reported the presence of the tetraspanin CD81 and the cytoplasmic protein TSG-101 in the EVs obtained from the dynamic condition, both also expressed from rat TSPCs-derived EVs culture in static conditions [6,8]. Further immunophenotypic characterisation of TSPCs-derived EVs showed the presence of several surface markers highly expressed in dynamic culture, such as CD63, CD9 and CD105, as also previously reported in hBM-MSCs-derived EVs [26], while two markers were only present in the static culture and two were equally expressed in both culture conditions (Figure 6c). Due to the high variability between all the human samples in their EVs-specific markers expression, no statistical significance was found. To overcome this issue, future prospects will include an increase in the sample number.

While our current study provides promising *in vitro* results in favour of using dynamic culture approaches for EV production from TSPCs, it is important to acknowledge some limitations. Firstly, although informative, our findings are based exclusively on *in vitro* research, which may not fully reflect the complex biological processes involved in tendon repair *in vivo*. Future research on tendon regeneration should include *in vivo* models to assess the therapeutic efficacy of EVs derived from TSPCs in a more realistic biological environment. Preclinical studies on tendon repair have demonstrated promising regenerative effects using EVs derived from tendon stem/progenitor cells of animal sources, including enhanced collagen synthesis, reduced scar formation, and improved tendon strength [19,77,78]. However, while EVs from other human stem cell sources, such as bone marrow [29] and adipose tissue [33], have been investigated in preclinical settings, studies specifically on EVs from human TSPCs remain limited. This gap represents an important research opportunity, and our future studies will focus on isolating and evaluating the therapeutic potential of human TSPC-derived EVs in tendon repair models. Such research will help establish the

safety, efficacy, and translational relevance of human TSPC-derived EVs as a potential therapeutic strategy for tendon disorders. Furthermore, expanding the sample size and investigating the specific mechanisms *via* which TSPCs-derived EVs contribute to tissue repair might provide crucial new perspectives on how to employ them most effectively in clinical applications. Regarding these mechanisms, though not yet fully defined, it is reasonable to speculate that the tetraspanins, present in human TSPC-derived EVs as we showed, could play a significant role in promoting tendon regeneration. These molecules have been shown in other studies to enhance processes critical to tissue repair, including extracellular matrix (ECM) remodelling, regulating EV biogenesis and cargo delivery, promoting cell adhesion and migration, and modulating immune responses [75,79]. Further investigation into these roles in the context of tendon repair may open new therapeutic options.

Additionally, when comparing static and dynamic culture systems, time and costs are important factors that must be considered. Although the initial setup costs of dynamic culture systems are higher, we showed they can provide a significantly higher efficiency in EV production. This enhanced efficiency over time may help to partially offset the initial investment, particularly in clinical translation, where large-scale EV production is essential. Consequently, dynamic systems, despite their complexity, may ultimately offer a more cost-effective solution in the long run by significantly enhancing EV output for therapeutic applications.

By addressing and tackling all these challenges in future studies, the therapeutic relevance of TSPC-derived EVs for tendon repair can be more effectively evaluated, translated and integrated into clinical practice.

Conclusions

Taken together, these data suggest that we developed an effective protocol to isolate EVs from human TSPCs using dynamic culture. By leveraging dynamic culture systems, we aimed to mimic the physiological microenvironment more accurately, thereby enhancing the production and quality of EVs derived from TSPCs compared to static culture methods. Furthermore, the larger protein content within the EVs isolated under dynamic culture conditions suggests a potential enrichment of bioactive molecules, including proteins and lipids, which are integral for cellular signalling and tissue regeneration processes. These enriched EVs hold promise for therapeutic applications in tendon regeneration and offer avenues for advanced biomimetic formulations. The prospect of utilising EVs and their constituents in therapeutic strategies represents a paradigm shift in regenerative medicine, offering targeted and efficient approaches for addressing tendon disorders. By harnessing the regenerative potential of EVs, researchers can explore novel avenues for the development of therapeutics that not only promote tissue repair but also mitigate inflammation and enhance overall tissue healing. However, even though our study shows the potential of dynamic culture for EV production from TSPCs and offers promising *in vitro* therapeutic applications for tendon repair,

it is crucial to acknowledge the limitations of this work. This study isolated and characterised EVs from TSPCs, using standard markers to confirm EV identity rather than to investigate specific regenerative roles associated with individual marker. In particular, further research is needed to fully elucidate the precise mechanisms driving enhanced EV production under dynamic culture conditions, as the study does not directly explore the molecular pathways involved. Moreover, the therapeutic efficacy and mechanisms of TSPC-derived EVs have yet to be validated *in vivo*. Future investigations involving animal models of tendon injury will be essential to validate these findings in a physiological context and to provide a more comprehensive understanding of the regenerative potential and mechanisms of TSPC-derived EVs.

Acknowledgements

This manuscript acknowledges COST Action TENET CA22170 (European Cooperation in Science and Technology) for supporting PhD short mobility.

Ethics approval statement

The study was conducted in accordance with the Declaration of Helsinki and approved by the Institutional Review Board of San Giovanni di Dio e Ruggi D'Aragona Hospital (Salerno, Italy) (Review Board prot./SCCE n. 151 achieved on 29 October 2020).

Informed consent statement

Informed consent was obtained from all subjects involved in the study. Written informed consent has been obtained from the patient(s) to publish this paper.

Author contributions

Conceptualisation, M.C., N.R.F. and G.D.P.; methodology, M.C., M.C.C., E.P.L., J.L., E.G.; validation, M.C., M.C.C. and G.D.P.; formal analysis, M.C., M.C.C. and G.D.P.; investigation, M.C.; resources, G.D.P.; data curation, M.C., M.C.C., T.P.D., N.M. and G.D.P.; writing-original draft preparation, M.C.; writing-review and editing, M.C.C., J.L., E.G., T.P.D., N.R.F., N.M. and G.D.P.; supervision, M.C.C., T.P.D., N.R.F. and G.D.P.; funding acquisition, G.D.P.; project administration, G.D.P.; All authors have read and agreed to the published version of the manuscript.

Disclosure statement

No potential conflict of interest was reported by the author(s).

Funding

This project has received funding from the European Union's Horizon 2020 Research and Innovation Program under the Marie Skłodowska-Curie grant agreement, No. 955685 (www.p4fit.eu).

ORCID

Marta Clerici  <http://orcid.org/0009-0009-8579-5271>

Maria Camilla Ciardulli  <http://orcid.org/0000-0003-1341-0394>

Erwin Pavel Lamparelli  <http://orcid.org/0000-0001-9700-5809>
 Joseph Lovecchio  <http://orcid.org/0000-0002-4721-1388>
 Emanuele Giordano  <http://orcid.org/0000-0002-8054-2875>
 Tina P. Dale  <http://orcid.org/0000-0001-9461-8220>
 Nicholas R. Forsyth  <http://orcid.org/0000-0001-5156-4824>
 Nicola Maffulli  <http://orcid.org/0000-0002-5327-3702>
 Giovanna Della Porta  <http://orcid.org/0000-0002-1426-0159>

Data availability statement

The data that support the findings of this study are available from the corresponding author upon reasonable request.

References

- Oliva F, et al. Achilles tendon rupture and dysmetabolic diseases: a multicentric, epidemiologic study. *J Clin Med*. 2022;11:3698. doi: [10.3390/jcm11133698](https://doi.org/10.3390/jcm11133698).
- Maffulli N, Cuzzo F, Migliorini F, et al. The tendon unit: biochemical, biomechanical, hormonal influences. *J Orthop Surg Res*. 2023;18(1):311. doi: [10.1186/s13018-023-03796-4](https://doi.org/10.1186/s13018-023-03796-4).
- Morita W, Dakin SG, Snelling SJB, et al. Cytokines in tendon disease. *Bone Joint Res*. 2017;6(12):656–664. doi: [10.1302/2046-3758.612.BJR-2017-0112.R1](https://doi.org/10.1302/2046-3758.612.BJR-2017-0112.R1).
- Arvind V, Huang AH. Reparative and maladaptive inflammation in tendon healing. *Front Bioeng Biotechnol*. 2021;9:719047. doi: [10.3389/fbioe.2021.719047](https://doi.org/10.3389/fbioe.2021.719047).
- Wang Y, He G, Tang H, et al. Aspirin inhibits inflammation and scar formation in the injury tendon healing through regulating JNK/STAT-3 signalling pathway. *Cell Prolif*. 2019;52(4):e12650. doi: [10.1111/cpr.12650](https://doi.org/10.1111/cpr.12650).
- Zhang M, Liu H, Cui Q, et al. Tendon stem cell-derived exosomes regulate inflammation and promote the high-quality healing of injured tendon. *Stem Cell Res Ther*. 2020;11(1):402. doi: [10.1186/s13287-020-01918-x](https://doi.org/10.1186/s13287-020-01918-x).
- Bi Y, Ehrichou D, Kilts TM, et al. Identification of tendon stem/progenitor cells and the role of the extracellular matrix in their niche. *Nat Med*. 2007;13(10):1219–1227. doi: [10.1038/nm1630](https://doi.org/10.1038/nm1630).
- Wang Y, He G, Guo Y, et al. Exosomes from tendon stem cells promote injury tendon healing through balancing synthesis and degradation of the tendon extracellular matrix. *J Cell Mol Med*. 2019;23(8):5475–5485. doi: [10.1111/jcmm.14430](https://doi.org/10.1111/jcmm.14430).
- Ciardulli MC, Scala P, Giudice V, et al. Stem cells from healthy and tendinopathic human tendons: morphology, collagen and cytokines expression and their response to T3 thyroid hormone. *Cells*. 2022;11(16):2545. doi: [10.3390/cells11162545](https://doi.org/10.3390/cells11162545).
- Ni M, Lui P, Rui YF, et al. Tendon-derived stem cells (TDSCs) promote tendon repair in a rat patellar tendon window defect model. *J Orthop Res*. 2012;30(4):613–619. doi: [10.1002/jor.21559](https://doi.org/10.1002/jor.21559).
- Tan C, Lui P, Lee YW, et al. Scx-Transduced Tendon-Derived Stem Cells (TDSCs) promoted better tendon repair compared to mock-transduced cells in a rat patellar tendon window injury model. *PLoS One*. 2014;9(5):e97453. doi: [10.1371/journal.pone.0097453](https://doi.org/10.1371/journal.pone.0097453).
- Ciardulli MC, Lovecchio J, Parolini O, et al. Fibrin scaffolds perfused with transforming growth factor- β 1 as an in vitro model to study healthy and tendinopathic human tendon stem/progenitor cells. *Int J Mol Sci*. 2024;25(17):9563. doi: [10.3390/ijms25179563](https://doi.org/10.3390/ijms25179563).
- Pinnarò V, Kirchberger S, König S, et al. Oxidized phospholipids regulate tenocyte function via induction of amphiregulin in dendritic cells. *Int J Mol Sci*. 2024;25(14):7600. doi: [10.3390/ijms25147600](https://doi.org/10.3390/ijms25147600).
- Li H, Li Y, Xiang L, et al. Therapeutic potential of GDF-5 for enhancing tendon regenerative healing. *Regen Ther*. 2024;26:290–298. doi: [10.1016/j.reth.2024.03.029](https://doi.org/10.1016/j.reth.2024.03.029).
- Fitzgerald MJ, Mustapich T, Liang H, et al. Tendon transection healing can be improved with adipose-derived stem cells cultured with growth differentiation factor 5 and platelet-derived growth factor. *Hand (N Y)*. 2023;18(3):436–445. doi: [10.1177/15589447211028929](https://doi.org/10.1177/15589447211028929).
- Chen S, Wang J, Chen Y, et al. Tenogenic adipose-derived stem cell sheets with nanoyarn scaffolds for tendon regeneration. *Mater Sci Eng C Mater Biol Appl*. 2021;119:111506. doi: [10.1016/j.msec.2020.111506](https://doi.org/10.1016/j.msec.2020.111506).
- Ciardulli MC, Marino L, Lamparelli EP, et al. Dose-response tendon-specific markers induction by growth differentiation factor-5 in human bone marrow and umbilical cord mesenchymal stem cells. *Int J Mol Sci*. 2020;21(16):5905. doi: [10.3390/ijms21165905](https://doi.org/10.3390/ijms21165905).
- Tan S-L, Chan C-K, Ahmad TS, et al. Growth differentiation factor 5(GDF5)-induced mesenchymal stromal cells enhances tendon healing. *Tissue Engin Part C: Methods*. 2024;30(10):431–442. doi: [10.1089/ten.tec.2024.0230](https://doi.org/10.1089/ten.tec.2024.0230).
- Connor DE, Paulus JA, Dabestani PJ, et al. Therapeutic potential of exosomes in rotator cuff tendon healing. *J Bone Miner Metab*. 2019;37(5):759–767. doi: [10.1007/s00774-019-01013-z](https://doi.org/10.1007/s00774-019-01013-z).
- Johnstone RM, Adam M, Hammond JR, et al. Vesicle formation during reticulocyte maturation. Association of plasma membrane activities with released vesicles (exosomes). *J Biol Chem*. 1987;262(19):9412–9420.
- Shao H, Im H, Castro CM, et al. New technologies for analysis of extracellular vesicles. *Chem Rev*. 2018;118(4):1917–1950. doi: [10.1021/acs.chemrev.7b00534](https://doi.org/10.1021/acs.chemrev.7b00534).
- Camussi G, Deregibus M-C, Bruno S, et al. Exosome/microvesicle-mediated epigenetic reprogramming of cells. *Am J Cancer Res*. 2011;1(1):98–110.
- Abels ER, Breakefield XO. Introduction to extracellular vesicles: biogenesis, RNA cargo selection, content, release, and uptake. *Cell Mol Neurobiol*. 2016;36(3):301–312. doi: [10.1007/s10571-016-0366-z](https://doi.org/10.1007/s10571-016-0366-z).
- Iraci N, Leonardi T, Gessler F, et al. Focus on extracellular vesicles: physiological role and signalling properties of extracellular membrane vesicles. *Int J Mol Sci*. 2016;17(2):171. doi: [10.3390/ijms17020171](https://doi.org/10.3390/ijms17020171).
- Citro V, Clerici M, Boccaccini AR, et al. Tendon tissue engineering: an overview of biologics to promote tendon healing and repair. *J Tissue Eng*. 2023;14:20417314231196275. doi: [10.1177/20417314231196275](https://doi.org/10.1177/20417314231196275).
- Chamberlain CS, Clements AEB, Kink JA, et al. Extracellular vesicle-educated macrophages promote early achilles tendon healing. *Stem Cells*. 2019;37(5):652–662. doi: [10.1002/stem.2988](https://doi.org/10.1002/stem.2988).
- Shen H, Yoneda S, Abu-Amer Y, et al. Stem cell-derived extracellular vesicles attenuate the early inflammatory response after tendon injury and repair. *J Orthop Res*. 2020;38(1):117–127. doi: [10.1002/jor.24406](https://doi.org/10.1002/jor.24406).
- Koay EJ, Athanasiou KA. Hypoxic chondrogenic differentiation of human embryonic stem cells enhances cartilage protein synthesis and biomechanical functionality. *Osteoarthritis Cartilage*. 2008;16(12):1450–1456. doi: [10.1016/j.joca.2008.04.007](https://doi.org/10.1016/j.joca.2008.04.007).
- Yu H, Cheng J, Shi W, et al. Bone marrow mesenchymal stem cell-derived exosomes promote tendon regeneration by facilitating the proliferation and migration of endogenous tendon stem/progenitor cells. *Acta Biomater*. 2020;106:328–341. doi: [10.1016/j.actbio.2020.01.051](https://doi.org/10.1016/j.actbio.2020.01.051).
- Li J, Liu Z-P, Xu C, et al. TGF- β 1-containing exosomes derived from bone marrow mesenchymal stem cells promote proliferation, migration and fibrotic activity in rotator cuff tenocytes. *Regen Ther*. 2020;15:70–76. doi: [10.1016/j.reth.2020.07.001](https://doi.org/10.1016/j.reth.2020.07.001).
- Huang Y, He B, Wang L, et al. Bone marrow mesenchymal stem cell-derived exosomes promote rotator cuff tendon-bone healing by promoting angiogenesis and regulating M1 macrophages in rats. *Stem Cell Res Ther*. 2020;11(1):496. doi: [10.1186/s13287-020-02005-x](https://doi.org/10.1186/s13287-020-02005-x).
- Shi Y, Shi H, Nomi A, et al. Mesenchymal stem cell-derived extracellular vesicles: a new impetus of promoting angiogenesis in tissue regeneration. *Cytotherapy*. 2019;21(5):497–508. doi: [10.1016/j.jcyt.2018.11.012](https://doi.org/10.1016/j.jcyt.2018.11.012).
- Shen H, Lane RA. Extracellular vesicles from primed adipose-derived stem cells enhance achilles tendon repair by reducing inflammation and promoting intrinsic healing. *Stem Cells*. 2023;41(6):617–627. doi: [10.1093/stmcls/sxad032](https://doi.org/10.1093/stmcls/sxad032).

- [34] Chen S-H, Chen Z-Y, Lin Y-H, et al. Extracellular vesicles of adipose-derived stem cells promote the healing of traumatized achilles tendons. *Int J Mol Sci.* 2021;22(22):12373. doi: [10.3390/ijms222212373](https://doi.org/10.3390/ijms222212373).
- [35] Li M, Jia J, Li S, et al. Exosomes derived from tendon stem cells promote cell proliferation and migration through the TGF β signal pathway. *Biochem Biophys Res Commun.* 2021;536:88–94. doi: [10.1016/j.bbrc.2020.12.057](https://doi.org/10.1016/j.bbrc.2020.12.057).
- [36] Kang H, Bae Y, Kwon Y, et al. Extracellular vesicles generated using bioreactors and their therapeutic effect on the acute kidney injury model. *Adv Healthc Mater.* 2022;11(4):e2101606. doi: [10.1002/adhm.202101606](https://doi.org/10.1002/adhm.202101606).
- [37] Watson DC, Bayik D, Srivatsan A, et al. Efficient production and enhanced tumor delivery of engineered extracellular vesicles. *Biomaterials.* 2016;105:195–205. doi: [10.1016/j.biomaterials.2016.07.003](https://doi.org/10.1016/j.biomaterials.2016.07.003).
- [38] Patel DB, Luthers CR, Lerman MJ, et al. Enhanced extracellular vesicle production and ethanol-mediated vascularization bioactivity via a 3D-printed scaffold-perfusion bioreactor system. *Acta Biomater.* 2019;95:236–244. doi: [10.1016/j.actbio.2018.11.024](https://doi.org/10.1016/j.actbio.2018.11.024).
- [39] Yuan X, Sun L, Jeske R, et al. Engineering extracellular vesicles by three-dimensional dynamic culture of human mesenchymal stem cells. *J Extracell Vesicles.* 2022;11(6):e12235. doi: [10.1002/jev.2.12235](https://doi.org/10.1002/jev.2.12235).
- [40] Almeria C, Kreß S, Weber V, et al. Heterogeneity of mesenchymal stem cell-derived extracellular vesicles is highly impacted by the tissue/cell source and culture conditions. *Cell Biosci.* 2022;12(1):51. doi: [10.1186/s13578-022-00786-7](https://doi.org/10.1186/s13578-022-00786-7).
- [41] Artuyants A, et al. Production of extracellular vesicles using a CELLline adherent bioreactor flask. In Turksen K, editor. *Bioreactors in stem cell biology: methods and protocols.* New York, NY: Springer US; 2022. p. 183–192. doi: [10.1007/978-1-4939-6728-5_413](https://doi.org/10.1007/978-1-4939-6728-5_413).
- [42] Lamparelli EP, Lovecchio J, Ciardulli MC, et al. Chondrogenic commitment of human bone marrow mesenchymal stem cells in a perfused collagen hydrogel functionalized with hTGF- β 1-releasing PLGA microcarrier. *Pharmaceutics.* 2021;13(3):399. doi: [10.3390/pharmaceutics13030399](https://doi.org/10.3390/pharmaceutics13030399).
- [43] Gardiner C, Di Vizio D, Sahoo S, et al. Techniques used for the isolation and characterization of extracellular vesicles: results of a worldwide survey. *J Extracell Vesicles.* 2016;5(1):32945. doi: [10.3402/jev.v5.32945](https://doi.org/10.3402/jev.v5.32945).
- [44] Clerici M, Citro V, Byrne AL, et al. Endotenon-derived type II tendon stem cells have enhanced proliferative and tenogenic potential. *Int J Mol Sci.* 2023;24(20):15107. doi: [10.3390/ijms242015107](https://doi.org/10.3390/ijms242015107).
- [45] Schneider CA, Rasband WS, Eliceiri KW. NIH Image to ImageJ: 25 years of image analysis. *Nat Methods.* 2012;9(7):671–675. doi: [10.1038/nmeth.2089](https://doi.org/10.1038/nmeth.2089).
- [46] Bustin SA, Benes V, Garson JA, et al. The MIQE guidelines: minimum information for publication of quantitative real-time PCR experiments. *Clin Chem.* 2009;55(4):611–622. doi: [10.1373/clinchem.2008.112797](https://doi.org/10.1373/clinchem.2008.112797).
- [47] Scala P, Lovecchio J, Lamparelli EP, et al. Myogenic commitment of human stem cells by myoblasts Co-culture: a static vs. a dynamic approach. *Artif Cells Nanomed Biotechnol.* 2022;50(1):49–58. doi: [10.1080/21691401.2022.2039684](https://doi.org/10.1080/21691401.2022.2039684).
- [48] Cortella G, Lamparelli EP, Ciardulli MC, Lovecchio J, Giordano E, Maffulli N, Della Porta G. ColMA-based bioprinted 3D scaffold allowed to study tenogenic events in human tendon stem cells. *Bioeng Transl Med.* 2025;10(1):e10723. doi: [10.1002/btm2.10723](https://doi.org/10.1002/btm2.10723).
- [49] Xu R, Simpson RJ, Greening DW. A protocol for isolation and proteomic characterization of distinct extracellular vesicle subtypes by sequential centrifugal ultrafiltration. In Hill AF, editor. *Exosomes and microvesicles: methods and protocols.* New York, NY: Springer; 2017. p. 91–116. doi: [10.1007/978-1-4939-6728-5_7](https://doi.org/10.1007/978-1-4939-6728-5_7).
- [50] Stam J, Bartel S, Bischoff R, et al. Isolation of extracellular vesicles with combined enrichment methods. *J Chromatogr B Analyt Technol Biomed Life Sci.* 2021;1169:122604. doi: [10.1016/j.jchromb.2021.122604](https://doi.org/10.1016/j.jchromb.2021.122604).
- [51] Citeroni MR, Ciardulli MC, Russo V, et al. In vitro innovation of tendon tissue engineering strategies. *Int J Mol Sci.* 2020;21(18):6726. doi: [10.3390/ijms21186726](https://doi.org/10.3390/ijms21186726).
- [52] Xu T, Xu M, Bai J, et al. Tenocyte-derived exosomes induce the tenogenic differentiation of mesenchymal stem cells through TGF- β . *Cytotechnology.* 2019;71(1):57–65. doi: [10.1007/s10616-018-0264-y](https://doi.org/10.1007/s10616-018-0264-y).
- [53] Lui PPY. Stem cell technology for tendon regeneration: current status, challenges, and future research directions. *Stem Cells Cloning.* 2015;8:163–174. doi: [10.2147/SCCAA.S60832](https://doi.org/10.2147/SCCAA.S60832).
- [54] Hao Z-C, Wang S-Z, Zhang X-J, et al. Stem cell therapy: a promising biological strategy for tendon–bone healing after anterior cruciate ligament reconstruction. *Cell Prolif.* 2016;49(2):154–162. doi: [10.1111/cpr.12242](https://doi.org/10.1111/cpr.12242).
- [55] Gupta A, Cady C, Fauser A-M, et al. Cell-free stem cell-derived extract formulation for regenerative medicine applications. *Int J Mol Sci.* 2020;21(24):9364. doi: [10.3390/ijms21249364](https://doi.org/10.3390/ijms21249364).
- [56] Ruzzini L, Abbruzzese F, Rainer A, et al. Characterization of age-related changes of tendon stem cells from adult human tendons. *Knee Surg Sports Traumatol Arthrosc.* 2014;22(11):2856–2866. doi: [10.1007/s00167-013-2457-4](https://doi.org/10.1007/s00167-013-2457-4).
- [57] Menon A, Creo P, Piccoli M, et al. Chemical activation of the hypoxia-inducible factor reversibly reduces tendon stem cell proliferation, inhibits their differentiation, and maintains cell undifferentiation. *Stem Cells Int.* 2018;2018:e9468085–13. doi: [10.1155/2018/9468085](https://doi.org/10.1155/2018/9468085).
- [58] Krampera M, Galipeau J, Shi Y, et al. Immunological characterization of multipotent mesenchymal stromal cells—The International Society for Cellular Therapy (ISCT) working proposal. *Cytotherapy.* 2013;15(9):1054–1061. doi: [10.1016/j.jcyt.2013.02.010](https://doi.org/10.1016/j.jcyt.2013.02.010).
- [59] Tan Q, Lui PPY, Rui YF. Effect of in vitro passaging on the stem cell-related properties of tendon-derived stem cells—implications in tissue engineering. *Stem Cells Dev.* 2012;21(5):790–800. doi: [10.1089/scd.2011.0160](https://doi.org/10.1089/scd.2011.0160).
- [60] Lui PPY, Chan KM. Tendon-Derived Stem Cells (TDSCs): From basic science to potential roles in tendon pathology and tissue engineering applications. *Stem Cell Rev Rep.* 2011;7(4):883–897. doi: [10.1007/s12015-011-9276-0](https://doi.org/10.1007/s12015-011-9276-0).
- [61] Zhang J, Wang JH-C. Characterization of differential properties of rabbit tendon stem cells and tenocytes. *BMC Musculoskelet Disord.* 2010;11(1):10. doi: [10.1186/1471-2474-11-10](https://doi.org/10.1186/1471-2474-11-10).
- [62] Rui Y-F, Lui PPY, Li G, et al. Isolation and characterization of multipotent rat tendon-derived stem cells. *Tissue Eng Part A.* 2010;16(5):1549–1558. doi: [10.1089/ten.TEA.2009.0529](https://doi.org/10.1089/ten.TEA.2009.0529).
- [63] Yin Z, Chen X, Chen JL, et al. The regulation of tendon stem cell differentiation by the alignment of nanofibers. *Biomaterials.* 2010;31(8):2163–2175. doi: [10.1016/j.biomaterials.2009.11.083](https://doi.org/10.1016/j.biomaterials.2009.11.083).
- [64] Bernard-Beaubois K, Hecquet C, Houcine O, et al. Culture and characterization of juvenile rabbit tenocytes. *Cell Biol Toxicol.* 1997;13(2):103–113. doi: [10.1023/b:cbto.0000010395.51944.2a](https://doi.org/10.1023/b:cbto.0000010395.51944.2a).
- [65] Yao L, Bestwick CS, Bestwick LA, et al. Phenotypic drift in human tenocyte culture. *Tissue Eng.* 2006;12(7):1843–1849. doi: [10.1089/ten.2006.12.1843](https://doi.org/10.1089/ten.2006.12.1843).
- [66] Liu Y, Suen C-W, Zhang J, et al. Current concepts on tenogenic differentiation and clinical applications. *J Orthop Translat.* 2017;9:28–42. doi: [10.1016/j.jot.2017.02.005](https://doi.org/10.1016/j.jot.2017.02.005).
- [67] Keller TC, Hogan MV, Kesturu G, et al. Growth/differentiation factor-5 modulates the synthesis and expression of extracellular matrix and cell-adhesion-related molecules of rat Achilles tendon fibroblasts. *Connect Tissue Res.* 2011;52(4):353–364. doi: [10.3109/03008207.2010.534208](https://doi.org/10.3109/03008207.2010.534208).
- [68] Tan S-L, Ahmad RE, Ahmad TS, et al. Effect of growth differentiation factor 5 on the proliferation and tenogenic differentiation potential of human mesenchymal stem cells in vitro. *Cells Tissues Organs.* 2012;196(4):325–338. doi: [10.1159/000335693](https://doi.org/10.1159/000335693).
- [69] Holladay C, Abbah S-A, O'Dowd C, et al. Preferential tendon stem cell response to growth factor supplementation. *J Tissue Eng Regen Med.* 2016;10(9):783–798. doi: [10.1002/term.1852](https://doi.org/10.1002/term.1852).
- [70] Park A, Hogan MV, Kesturu GS, et al. Adipose-derived mesenchymal stem cells treated with growth differentiation factor-5 express tendon-specific markers. *Tissue Eng Part A.* 2010;16(9):2941–2951. doi: [10.1089/ten.tea.2009.0710](https://doi.org/10.1089/ten.tea.2009.0710).

- [71] Govoni M, Berardi AC, Muscari C, et al. *An engineered multiphase three-dimensional microenvironment to ensure the controlled delivery of cyclic strain and human growth differentiation factor 5 for the tenogenic commitment of human bone marrow mesenchymal stem cells. *Tissue Eng Part A*. 2017;23(15–16):811–822. doi: [10.1089/ten.TEA.2016.0407](https://doi.org/10.1089/ten.TEA.2016.0407).
- [72] Youngstrom DW, LaDow JE, Barrett JG. Tenogenesis of bone marrow-, adipose-, and tendon-derived stem cells in a dynamic bioreactor. *Connect Tissue Res*. 2016;57(6):454–465. doi: [10.3109/03008207.2015.1117458](https://doi.org/10.3109/03008207.2015.1117458).
- [73] Han TTY, Walker JT, Grant A, et al. Preconditioning human adipose-derived stromal cells on decellularized adipose tissue scaffolds within a perfusion bioreactor modulates cell phenotype and promotes a pro-regenerative host response. *Front Bioeng Biotechnol*. 2021;9:642465. doi: [10.3389/fbioe.2021.642465](https://doi.org/10.3389/fbioe.2021.642465).
- [74] Syromiatnikova V, Prokopeva A, Gomzikova M. Methods of the large-scale production of extracellular vesicles. *Int J Mol Sci*. 2022; 23(18):10522. doi: [10.3390/ijms231810522](https://doi.org/10.3390/ijms231810522).
- [75] Jankovičová J, Sečová P, Michalková K, et al. Tetraspanins, more than markers of extracellular vesicles in reproduction. *Int J Mol Sci*. 2020;21(20):7568. doi: [10.3390/ijms21207568](https://doi.org/10.3390/ijms21207568).
- [76] Welsh JA, Goberdhan DCI, O'Driscoll L, et al. Minimal information for studies of extracellular vesicles (MISEV2023): From basic to advanced approaches. *J Extracell Vesicles*. 2024;13(2):e12404. doi: [10.1002/jev2.12404](https://doi.org/10.1002/jev2.12404).
- [77] Song K, Jiang T, Pan P, et al. Exosomes from tendon derived stem cells promote tendon repair through miR-144-3p-regulated tenocyte proliferation and migration. *Stem Cell Res Ther*. 2022;13(1):80. doi: [10.1186/s13287-022-02723-4](https://doi.org/10.1186/s13287-022-02723-4).
- [78] Zou M, Wang J, Shao Z. Therapeutic potential of exosomes in tendon and tendon–bone healing: a systematic review of preclinical studies. *J Funct Biomater*. 2023;14(6):299. doi: [10.3390/jfb14060299](https://doi.org/10.3390/jfb14060299).
- [79] Kooijmans SAA, de Jong OG, Schiffelers RM. Exploring interactions between extracellular vesicles and cells for innovative drug delivery system design. *Adv Drug Deliv Rev*. 2021;173:252–278. doi: [10.1016/j.addr.2021.03.017](https://doi.org/10.1016/j.addr.2021.03.017).